Jurnal Nasional Teknik Elektro dan Teknologi Informasi
Volume 13 Number 2 May 2024

DOI: 10.22146/jnteti.v13i2.10131

Electric Boat Propulsion with IPM BLDC Motors: Performance and Efficiency Analysis

Dewi Rianti Mandasari[1,2], Budi Sudiarto[1], Lia Amelia[2], Cuk Supriyadi Ali Nandar[3]

[1] Electrical Engineering Department, Faculty of Engineering, Universitas Indonesia, Depok, Jawa Barat 16424, Indonesia
[2] Research Center for Process and Manufacturing Industry Technology, National Research and Innovation Agency of the Republic of Indonesia, Serpong, Banten, 15314, Indonesia
[3] Research Center for Energy Conversion and Conservation, National Research and Innovation Agency of the Republic of Indonesia, Serpong, Banten, 15314, Indonesia

[Received: 3 November 2023, Revised: 5 January 2024, Accepted: 1 March 2024]
Corresponding Author: Dewi Rianti Mandasari (email: dewi031@brin.go.id)

ABSTRACT — Air pollution, particularly the presence of PM2.5 particles, remains a global health concern. While Indonesia exhibits lower PM2.5 levels than the global average, vehicular emissions significantly contribute to air pollution. In light of environmental and health considerations, adopting eco-friendly electric motors, mainly interior permanent magnet brushless direct current (IPM BLDC) motors, represents a promising solution for cleaner and more efficient boat propulsion systems, benefiting both the environment and the livelihoods of fishermen. This study thoroughly examines the efficiency and performance of IPM BLDC motors in boat propulsion, utilizing finite element analysis (FEA) through ANSYS Maxwell. The FEA simulations in ANSYS Maxwell were tailored to focus on crucial design variables such as motor torque, speed, and thermal management. It aimed to ensure that the motor specifications meet electric boats' operational needs in fishing and search operations. Notably, at the desired speed of 5,000 rpm, the motor achieved a torque of 15 Nm with a cogging torque of just 7% and maintained an average efficiency of 89%. Significantly, it operated at a safe temperature without requiring additional cooling systems. Furthermore, simulation outcomes suggested that the motor could effectively function at higher speeds, specifically 6,300 rpm, presenting an exciting opportunity to enhance boat propulsion systems through increased motor speed.

KEYWORDS — Ansys Maxwell, Air Pollution, BLDC Motors, Cogging Torque, Electric Boat, FEA, IPM-V.

I. INTRODUCTION

Air pollution has become a prominent topic of discussion worldwide. According to the World Health Organization (WHO), the PM2.5 parameter is the most influential air pollutant parameter affecting human health, with an air quality guideline of 10 µg/m³ [1]. According to the State of Global Air report for 2020, air pollution has risen yearly. In 2019, the global PM2.5 concentration was 42.6 µg/m³ [2]. In contrast, Indonesia registered a 19.4 µg/m³ concentration in the same year. Notably, 19% of the pollution in Indonesia is attributed to vehicular sources [3], primarily stemming from vehicle exhaust emissions utilizing fossil fuels [4]. Based on research data, when viewed from the perspective of fossil fuel production and availability, there was a significant decline in 2020 [5]. Fossil fuel production experienced a sharp decrease in 2020 compared to 2019, declining by 5%. All fossil fuels were affected, particularly oil, which saw a 7% decrease due to reduced transportation demand during the global health crisis.

Due to the long-standing use of fossil fuels as a source of propulsion for land, water, and air vehicles, most vehicles today still rely on nonrenewable fuels. One example is using diesel engines in boats powered by diesel fuel. The utilization of diesel engine fuel has both negative economic and health-related consequences. The frequent scarcity of diesel fuel can detrimentally affect fishermen, while the pollutant gases emitted by diesel engines and the noise, they generate pose health hazards to these individuals [6]. Hence, it is imperative to transition from diesel engines powered by diesel fuel to alternative propulsion systems that are more environmentally friendly and do not endanger fishermen's health. One such alternative is the adoption of electric motors for water transportation (boats).

Over time, the utilization of enhancement techniques to optimize the performance of electric machines, which serve as invaluable electrical tools, has emerged as a critical strategy for tackling this challenge [7]. Adopting permanent magnets in machines has garnered considerable attention from researchers and electric motor manufacturers. Permanent magnet machines can be categorized into two primary types: radial flux and axial flux [8]. Axial flux permanent magnet motors offer distinct advantages of high-power density, efficiency, and rapid dynamic response, all within a more compact form factor than radial flux. Radial flux permanent magnet motors have remarkable power and torque density while providing ease of speed control [9]. Moreover, their construction is relatively straightforward, making them an attractive choice for development and manufacturing in Indonesia.

Among the radial flux permanent magnet motor variants, permanent magnet brushless direct current (PM BLDC) motors have gained prominence as the preferred option for automotive applications due to their high efficiency and good reliability [9], [10], [11]. PM BLDC motors also deliver substantial torque across a broad spectrum of speeds, positioning them as advantageous alternatives to traditional brushed dc motors and induction motors when applied in the context of electric vehicles, especially in water transportation [12], [13]. The interior permanent magnet brushless dc (IPM BLDC) motor is designed with permanent magnets embedded within the rotor core, which makes both magnet torque and reluctance torque achieve elevated power density compared to traditional designs [14], [15], [16]. Additionally, it provides an extensive range of operating speeds by implementing field weakening control. The lack of familiarity among local electric motor manufacturers with the design of electric motors incorporating permanent magnets, coupled with limited access to materials,

TABLE I
OUTBOARD MOTOR PARAMETER

Parameter	Value	Unit
Max output	11 (15)	kW (hp)
Full throttle operating range	4,500–5,000	rpm
Cooling system	Water	-
Torque propeller shaft on 2,500 rpm	29.43	Nm
Torque Engine on 5,000 rpm	14.57	Nm

notably permanent magnets, within the Indonesian market, poses a significant challenge to domestic manufacturers' advancement of BLDC motor products.

This study aims to evaluate the effectiveness of BLDC motors for water transportation to achieve performance that adheres to the boat's specifications, ensures high efficiency, and prevents overheating with a design that is simple to produce by regional manufacturers in Indonesia. The outcomes of the performance simulations, such as torque, cogging torque, stator current, output, and input power, including efficiency and motor temperature, can serve as valuable references or points of consideration when formulating the boat's electrical or power supply system. This endeavor supports the internal combustion engine (ICE)-to-electric conversion initiative to mitigate pollution levels in Indonesia.

II. DESIGN REQUIREMENT

According to the Indonesian Capture Fisheries Statistics, fishing boat categories and sizes are distinguished based on two main categories for each type of fishing gear: nonpowered boats and powered boats or ships [17]. Powered boats with outboard motors are categorized by size, ranging from < 5 gt to over 1,000 gt. This study focuses on boats with less than 5 gt capacity equipped with outboard motors producing less than 15 hp. The specifications of the outboard motors utilized are detailed in Table I [18].

To align with the specific requirements of the existing outboard motor installed on the boat slated for conversion, adopting an IPM BLDC motor could be the optimal choice for serving as a propulsion unit. The IPM BLDC motor has advantages for its efficiency, reliability, and good power-to-weight ratio. Additionally, the inclusion of a permanent magnet embedded within the rotor structure endows the IPM BLDC motor with the capacity to generate more torque across a broad spectrum of operational speeds. The strategic configuration of the permanent magnet within a V-shaped arrangement optimizes the magnetic field's strength and allows for a greater magnetic volume [19]. This arrangement empowers the IPM BLDC motor to deliver elevated torque output, effectively meeting the required performance expected of an electric boat motor.

The rotor of the IPM BLDC produces a magnetic field that rotates at a steady frequency. Continuous use or exposure to vehicle loads beyond specified limits increases heat within the motor [19]. This temperature rise can diminish motor performance and potentially damage the insulation of the motor's windings, posing the risk of overheating.

Reducing the heat generated due to motor load and maximum speed usage is critical in electric motor design. Several factors contribute to poor heat dissipation in motors, including elevated operating temperatures, the working environment, installation space, and challenges in increasing power and torque density. Efforts to reduce motor temperature require innovative casing designs. Existing studies have primarily focused on cooling systems utilizing mediums like water, air, fluids, and oil. Water cooling and fan-based systems have shown positive effects on cooling BLDC motors.

Oil cooling provides excellent stator core cooling, extending performance at rated conditions [20]. A feasible substitute is to add fins to the electric motor's housing; these fins increase the rate of heat transfer and help to reduce the end windings' temperature [21]. This study evaluates the motor's operational durability through one hour of fishing and two hours of searching. To reduce propulsion system weight, fishing vessels with a gross tonnage under 5 gt use electric motors with tiny motor designs. The motor's design requires an IP rating of 67 to protect it from seawater splashes in an open environment. An electric motor with natural air cooling is excellent for boat propulsion.

III. DESIGN OF PM BLDC MOTOR

The PM BLDC motor design began with choosing a traction machine and boat thruster working conditions. Due to high torque at high speeds and a natural cooling system, a high torque density motor was needed.

An exhaustive literature analysis found PM BLDC motors acceptable due to their power density, efficiency, and torque capacity. The interior permanent magnet (IPM) motor and the surface permanent magnet (SPM) motor are two frequently utilized PM BLDC motors in traction applications. Comparing IPM and SPM motors involves various parameters [22].

Over SPM motors, IPM motors have superior power density, efficiency, and torque. The embedded or buried magnet rotor design of IPM motors maximizes magnet use and power output per volume [22]. IPM motors are more efficient at high speeds due to better flux distribution and magnet location [23].

IPM motors feature less torque ripple than SPM motors. IPM motor magnet arrangements—particularly flat-type and V-shape configurations—reduce cogging torque and provide smoother performance, especially at high speeds [22]. Electrical machine topology is presented in Figure 1 [24].

According to recent research investigations, The V-shape magnet design is becoming more and more popular in traction applications such as electric boat propulsion [25]. Substantial experimental data show that the V-shape configuration's accurate magnet distribution lowers cogging torque. By reducing magnetic field changes during rotor rotation, this configuration results in torque output that is more evenly distributed throughout every rotation. The V-shape arrangement has higher torque density than other layouts. In traction applications, high torque output per unit volume is required. V-shape arrangement experiments show better efficiency at various running speeds. The speed demands of boat thrusters fluctuate during maneuvering; therefore, this versatility fits. According to the explanations, this research's permanent magnet motor is an IPM V-shape BLDC motor (IPM-V motor).

The design process began with motor configuration, determining the IPM-V motor arrangement. Factors like pole count, stator and rotor dimensions, and magnet arrangement were analyzed to optimize power, efficiency, and torque. After motor configuration, the winding design focused on turn count and stator winding arrangement, significantly affecting voltage

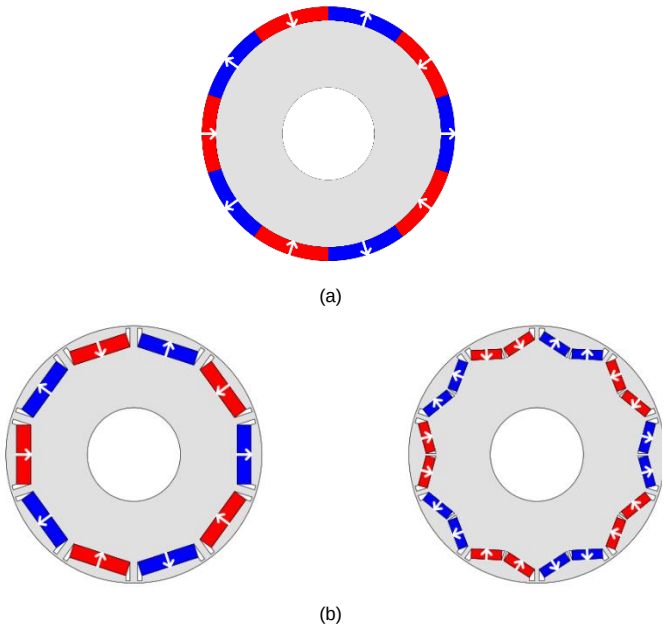

Figure 1. BLDC motor's topology, (a) SPM, (b) flat type and V-shape IPM.

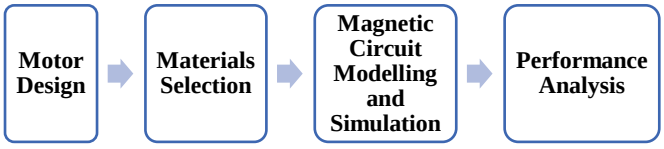

Figure 2. Design procedure of the BLDC motor utilizes Ansys Maxwell.

and current characteristics. Various winding configurations were explored for optimal performance.

Based on available materials, motor performance must be optimized. The next step is magnetic circuit modelling and simulation, where finite element analysis (FEA) analyzes a full model to evaluate magnetic flux, field strength, and losses to improve design parameters. Performance analysis evaluates input and output power, torque, efficiency, and thermal issues to ensure genuine performance. The methodology used in the design of a BLDC motor utilizing Ansys Maxwell is illustrated in Figure 2.

This study focused on the analysis of a IPM V-shape motor through FEA. FEA is method for modelling and simulating various parameter of an electric motor. It enables the representation of the motor's geometric configuration and understanding of complex interactions among magnetic fields, coils, and other components [26].

A. IPM-V MOTOR DESIGN

In this section, IPM V-shape motor component is designed and calculated including rotor core, stator core, and winding.

1) ROTOR

The arrangement of magnets on the rotor can influence the magnetic field distribution and flux linkage with the stator, thereby impacting torque, back electromotive force (EMF), and output power [22]. Torque and magnetic flux distribution can also be influenced by the pole shape of the rotor. The calculation for rotor diameter (D_r) [27] can refer to (1).

$$T = kD_rL \tag{1}$$

where T represents torque, k is a constant, and L is the axial length of the motor. From (1), the rotor diameter and motor length corresponding to the targeted torque can be determined.

2) STATOR

The design of the stator including its geometry and winding arrangement. Stator geometry parameters, such as the number of slots, slot dimensions, core shape, and yoke dimensions, are essential for ensuring the optimal magnetic flux distribution, minimizing magnetic losses, and enhancing motor performance [28].

The stator slot design needs to determine both size and shape. The stator slots that accommodate the stator windings impact magnetic flux distribution within the machine. Consequently, the choice of slot design significantly influences critical parameters, including the winding space factor, magnetic saturation, and copper losses. Different slot configurations, such as round, rectangular, or trapezoidal shapes, can be evaluated to determine the most suitable design [29]. The inner stator diameter (D_{is}) [27] refers to (2):

$$D_{is} = D_r + 2\delta \tag{2}$$

where δ represents the airgap. Determining the outer stator diameter also considers the inner stator diameter and the available space within the boat engine casing.

The stator design includes the stator tooth design. The stator tooth width (t) [30] is defined by (3):

$$t = \tau \times \lambda \tag{3}$$

where λ represents the tooth pitch and τ is the ratio of tooth width to slot pitch (sloth-pitch).

Generally, BLDC motors exhibit three distinct types of torque: mutual, reluctance, and cogging. Cogging torque, which arises from the interaction between permanent magnets (PM) embedded in the rotor and the stator slots, is an inherent characteristic of BLDC motors, particularly those with an IPM-V motor configuration [31].

Different methods have been used in stator slot design to reduce cogging torque. It involves eliminating slots, employing skewed or irregularly shaped slots, and meticulously selecting the number of slots and poles. Effective design practices have demonstrated the potential for cogging torque reduction [32].

The parameters of interest, namely the number of slots (N_s) and skew angle (α_{sk}) [33], can be determined using (4).

$$\alpha_{sk} = \frac{360^0}{N_s N_{period}}. \tag{4}$$

The single-slot pitch cogging torque period is N_{period} . Equation (4) shows the relationship between N_{period} and the ideal skew angle to minimize cogging torque.

A single slot pitch's cogging torque period is N_{period} [33]. Equation (5) explains how N_{period} affects the ideal skew angle for cogging torque minimization. The highest common factor between poles and stator slots is *HCF*.

$$N_{period} = \frac{N_p}{HCF(N_s, N_p)}. \tag{5}$$

Using (3) and (4), a skew angle of 15° was calculated for the IPM-V motor with 12 stator slots and 8 poles. Implementing a 15° skew angle may complicate and increase manufacturing costs.

According to previous studies, BLDC motors with skew angles between 6° and 15° maintain cogging torque below 10% of the rated torque [34]. Based on this concept, this research carried out theoretical analysis and exact calculations for a BLDC motor with 12 stator slots and 8 poles. A compromise

TABLE II
MOTOR DESIGN PARAMETER

No	Parameter	Value	Unit
1	Motor type	BLDC IPM V-Shape	-
2	Input voltage	72	Vdc
3	Number of phases	3	-
4	Number of slots	12	-
5	Number of poles	8	-
6	Stator outer diameter	175	mm
7	Rotor outer diameter	98.8	mm
8	Lamination length	105	mm
9	Skew stator	10	°
10	Magnet thickness	3	mm
11	Magnet width	14.3	mm

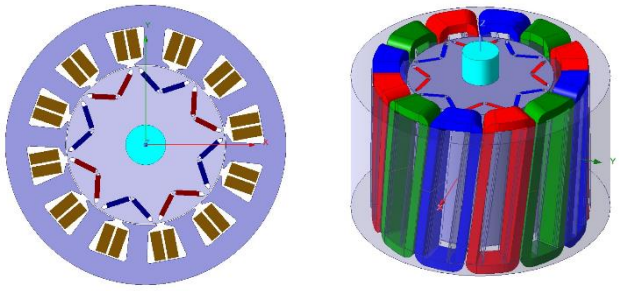

(a) (b)

Figure 3. Design of IPM-V motor, (a) 2D and (b) 3D.

between increased performance and production efficiency is aimed. A maximum cogging torque limit of 10% of the rated torque was established in the investigation with inclination angles ranging from 6° to 15° [34].

The research recommends motors with skew angles between 6° and 15° considering to manufacturing simplicity. The approach of this range reduces cogging torque while simplifying manufacture [34]. This strategy affects a reasonable balance between theoretical understanding and practical manufacturing limitations.

3) WINDING

Winding arrangement refers to the stator windings distributed within the slots. There are two common winding arrangements: concentrated winding and distributed winding. Concentrated windings have all the windings in one slot, while distributed windings divide the windings among several slots. The choice of winding arrangement impacts factors such as the winding factor, copper losses, and electromagnetic performance. Choosing a winding arrangement that suits the motor's specific needs and optimizes the magnetic field distribution is crucial [35].

The integer portion uses the following calculation to determine the nominal coil span [27] in the slot:

$$S = max\left(fix\left(\frac{N_s}{p}\right), 1\right) \quad (6)$$

where N_s is the number of stator slots and p is the number of poles. The *max(.,.)* function ensures that when the number of stator slots is less than the number of poles, the coil span value is at least one slot.

After performing the calculation, it was decided to employ a distributed winding arrangement for the IPM-V motor. The parameters for the motor design are presented in Table II.

TABLE III
MATERIAL OF BLDC MOTOR

No	Item	Material
1	Core stator	50JN1300
2	Core rotor	50JN1300
3	Wire	Copper
4	Permanent magnet	NdFe52 (up to 120˚C)
5	Insulation class	H

The design of the IPM-V motor was obtained from the stator, windings, rotor, and permanent magnet designs, as illustrated in Figure 3.

B. MATERIAL SELECTION

To improve performance and longevity, the electric boat IPM-V motor employed carefully selected materials for critical components. The stator core, a motor component, was made of high-quality, laminated electrical steel sheets with low core losses. The material used for the stator and rotor core was 50JN1300 since the material characteristics are suitable for electric motors, such as high magnetic permeability, good electrical conductivity, and strong mechanical strength. Those parameters make 50JN1300 suitable for ensuring efficient energy conversion and durability in electric motor operation. The rotor slots were inserted with permanent magnets using NdFeB material, known as neodymium magnets of the NdFe52 type, which have advantages in their magnetic properties, such as high magnetic strength and coercivity. These magnets have been widely used in high-performance devices and vehicle propulsion systems [36]. Table III shows the results of material selection.

C. MAGNETIC CIRCUIT MODELLING AND SIMULATION

Electromagnetic simulation aiming to obtain and analyze various parameter by using Ansys Maxwell, such as torque, cogging torque, current, output and input power, efficiency, magnetic field distribution and motor temperature.

1) TORQUE

Ansys Maxwell estimates electromagnetic torque by modelling stator-rotor electromagnetic interactions. Torque characteristics are predicted exactly using magnetic field strength, rotor position, and winding current.

2) COGGING TORQUE

Ansys Maxwell can simulate cogging torque by examining the permanent magnets on the rotor and on the stator teeth. It helps identify motor design cogging concerns.

3) CURRENT

The current distribution in motor windings under various load and speed conditions can be simulated by Ansys Maxwell. It details current behavior by considering electromagnetic induction and resistance.

4) OUTPUT POWER

FEA calculates output power by simulating motor mechanical interactions like rotor rotation and load work. This approach evaluates motor mechanical output. The motor's output power can be calculated from Ansys Maxwell simulation torque and speed versus time data (7).

$$P_{out} = S \times T \quad (7)$$

where S represents rotation speed in rpm, and T represents torque in Nm.

5) INPUT POWER

FEA offers the capability to model the input power of the motor, quantifying losses in the magnetic circuit, winding copper losses, and core losses to estimate the overall input power under various operating conditions. In Ansys Maxwell software, (8) and (9) calculate the input power.

$$P_{TotalLoss} = P_{CoreLoss} + P_{StrandedLoss} \quad (8)$$

$$P_{in} = P_{out} + P_{Total\ Loss} \quad (9)$$

$P_{TotalLoss}$ represents the total loss in the electromagnetic simulation, which includes core loss denoted by $P_{CoreLoss}$ and copper loss denoted by $P_{StrandedLoss}$. It followed by the calculation of input power, achieved by summing (7) and (8).

6) EFFICIENCY

The motor's efficiency can be assessed through the results of FEA simulations by dividing the output power by the input power, as shown in (10).

$$Eff = \frac{P_{out}}{P_{in}} \times 100\%. \quad (10)$$

7) MAGNETIC FIELD DISTRIBUTION

Ansys Maxwell excels at visualizing and analyzing the magnetic field distribution within the motor. It includes assessing flux density, which is crucial for optimizing motor performance.

8) MOTOR TEMPERATURE

FEA can be utilized for thermal analysis by considering material properties, heat generation due to losses, and heat transfer mechanisms within the motor. This method enables the prediction of temperature distribution, ensuring that the motor operates within safe thermal limits [37].

IV. RESULT AND ANALYSIS

IPM-V motor simulation results were comprehensively analyzed for performance and efficiency. The performance evaluation measures how well the IPM-V motor design meets design objectives. Conversely, the efficiency assessment used software FEA simulation results to evaluate the motor's efficiency.

The results of this comprehensive investigation are representative because it used averaged data from stable motor operation. The simulation output parameters include torque, cogging torque, current, output power, input power, efficiency, and magnetic field distribution. The FEA simulations include targeted and maximum speeds. The analysis at the targeted speed evaluates motor performance under conditions similar to existing internal combustion engines, while the analysis at maximum speed examines the motor's potential and performance in developing propulsion systems for boats using existing engines.

This research estimated motor temperature using simulations in addition to performance and efficiency metrics. Speed and motor duration were used to assess temperature changes. These simulation scenarios were based on a deep understanding of real-world electric boat operations, including fishing and fish finding.

1) TORQUE

In propulsion systems, one of the crucial parameters that a motor must meet in delivering performance is torque. In this research, the torque parameter of the IPM-V motor was analyzed based on the requirements of the boat propulsion system. The torque of the IPM-V motor is shown in Figure 4.

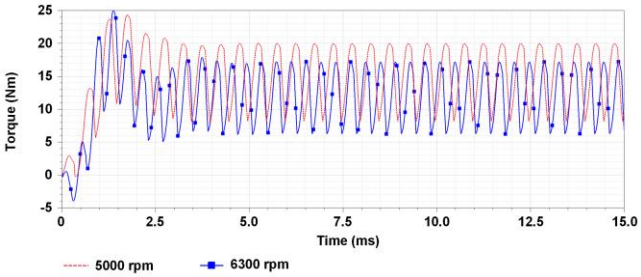

Figure 4. The torque curve of IPM-V motor.

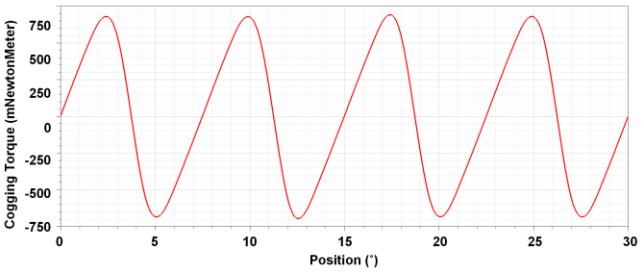

Figure 5. The cogging torque curve of IPM-V motor.

Upon achieving a stable operational state, occurring after a duration of 5 ms, it was observed that the average torque at 5,000 rpm stood at 15.15 Nm. Meanwhile, at 6,300 rpm, the average torque registered 12.19 Nm. Compared to the torque requisites for electric boat traction, the motor produced approximately 15 Nm of torque at 5,000 rpm, whereas at 6,300 rpm, the torque generated approximates 11.9 Nm. Consequently, it may be inferred that this IPM-V motor satisfactorily complies with the specified torque criteria for electric boat propulsion applications.

2) COGGING TORQUE

Cogging torque is the periodic torque that manifests when a BLDC motor's rotor is in motion. Implementing a 10° skew angle on the stator aims to reduce the torque to below 10% of the rated or maximum torque. The curve of cogging torque is shown in Figure 5.

The simulations yielded a peak-to-peak cogging torque measurement of 1.386 Nm while considering a rated torque of 15.15 Nm, resulting in a cogging torque percentage of approximately 8.49%. These results are in accordance with the predetermined target, which stipulates that cogging torque should remain below 10% of the rated torque.

3) STATOR CURRENT

Stator current refers to the flow of electric current through the stator of an IPM-V motor, which constitutes the stationary, nonrotating component of the motor. Stator current serves the purpose of creating a magnetic field within the stator, and this magnetic field interacts with the rotor to generate mechanical motion. The stator current consists of three phases that drive the rotation process. Consequently, examining the stator current holds significance in comprehending alterations in the magnetic field's intensity and polarity during motor rotation. The stator current curve can be seen in Figure 6.

Figure 6 shows that when operating at 5,000 rpm, the IPM-V motor produced a torque of 15.15 Nm under stable conditions, requiring an average current of 102.48 A and a maximum current of 176.85 A. Whereas at 6,300 rpm, to generate a torque of 12.19 Nm, an average current of 114.16 A was needed with a maximum current of 196.38 A. The waveform of the stator current in Figure 6 shows a balanced distribution among the

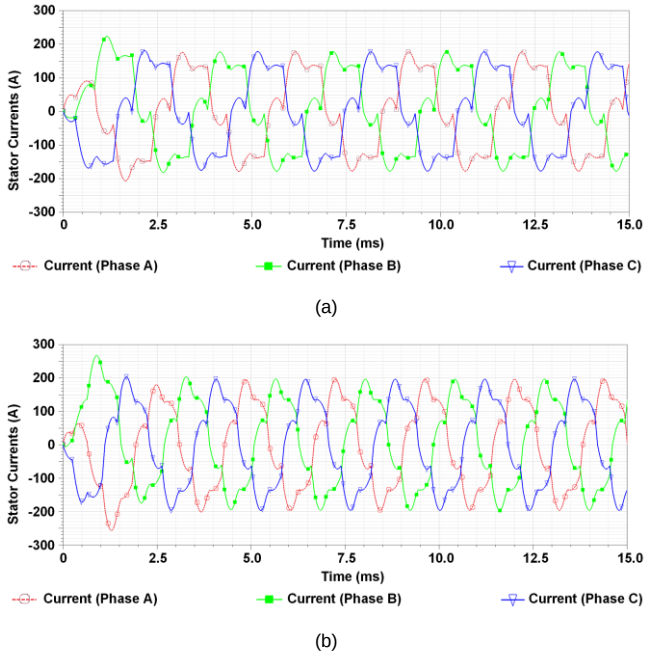

Figure 6. The current curve of IPM-V motor, (a) 5,000 rpm, (b) 6,300 rpm.

three phases. This balance affected the polarity of the magnetic field and the smoothness of the motor's rotation. These simulation results indicate that higher rotational speeds demand higher current levels. These simulation results can serve as a recommendation for selecting the appropriate batteries for electric boat thrusters.

4) OUTPUT POWER

Mechanical power generated by the interaction between the magnetic field and the magnetic material within the motor can be quantified. Analyzing mechanical power is essential for comprehending the magnitude of the output power produced by the electric motor. The generated mechanical power can be calculated by multiplying the motor's rotational speed data by the motor's torque. The power output curve is displayed in Figure 7. The power output curve is displayed in Figure 7 for 5,000 rpm and 6,300 rpm speed.

Electric motor output power was calculated when the electric motor's rotation had stabilized, namely after 5 ms. The average output power obtained at a motor speed of 5,000 rpm was 7.93 kW, and at 6,300 rpm was 8.04 kW.

5) INPUT POWER

The analysis of input power in the IPM-V motor was performed using the predefined method discussed in Section III by summing the output power and losses. The losses considered in the electromagnetic-based FEA were core losses and stranded losses. Based on the results from FEA simulations, the input power values are shown in Figure 7.

Electric motor input power was calculated when the electric motor's rotation stabilized after 5 ms. The average input power obtained at a motor speed of 5,000 rpm was 8.82 kW, while at 6,300 rpm, it was 8.95 kW.

6) EFFICIENCY

Efficiency in the IPM-V motors refers to the motor's ability to convert input power, which is the total power absorbed by the motor from the electrical energy source, into output power in the form of mechanical power in the form of torque and rotation. The efficiency calculation results are presented in Figure 8.

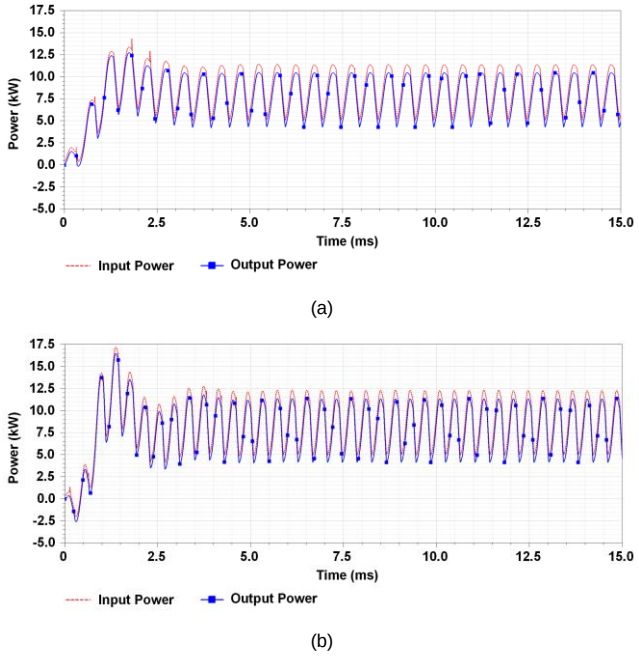

Figure 7. The input and output power curve of IPM-V motor, (a) 5,000 rpm, (b) 6,300 rpm.

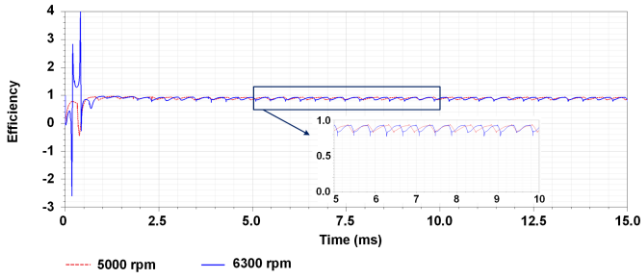

Figure 8. The efficiency curve of IPM-V motor.

Electric motor efficiency was calculated when the electric motor's rotation had stabilized, occurring after 5 ms. The average efficiency obtained at a motor speed of 5,000 rpm was 89.34%, with a minimum value of 82.32% and a maximum value of 94.28%. At a motor speed of 6,300 rpm, the average efficiency was 88.90%, with a minimum value of 77.17% and a maximum value of 93.65%. Higher motor efficiency indicates a more excellent electrical power conversion into useful mechanical power. It can be observed that an increase in speed leads to a decrease in efficiency, primarily due to increased losses.

7) MAGNETIC FIELD DISTRIBUTION

The magnetic field plot generated illustrates the pattern and intensity of the magnetic field at various parts of the motor. An even and concentrated magnetic field distribution in the desired area indicates an effective permanent magnet design for generating the required magnetic field for energy conversion. The simulation results of magnetic field distribution are presented in Figure 9.

Based on the results of FEA simulations, at a rotational speed of 5,000 rpm, the highest flux density obtained was 2.492 T in the rotor and 2.09 T in the stator, while at a rotational speed of 6,300 rpm, the highest flux density obtained was 2.526 T in the rotor and 2.11 T in the stator.

These simulation findings indicate that higher rotational speeds result in an increase in flux density within the motor. High flux density can lead to an increase in the heat energy generated within the motor. It can result in higher motor

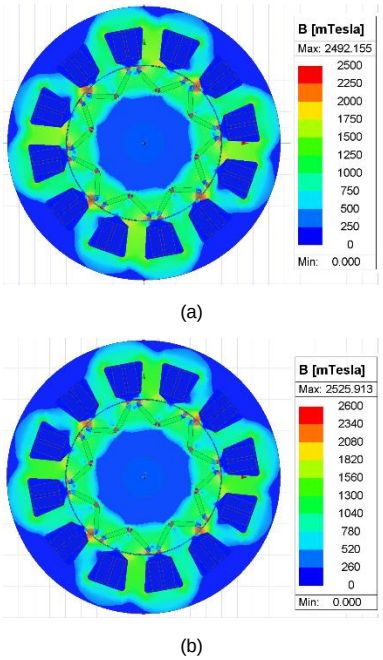

Figure 9. Magnetic field distribution graph, (a) 5,000 rpm, (b) 6,300 rpm.

temperatures [38]. Elevated temperatures can accelerate the ageing process of various motor components, such as winding wires, insulation, and permanent magnets. Therefore, it is necessary to analyze the motor temperature as a consequence of the high flux density in the motor.

8) MOTOR TEMPERATURE

The utilization of IPM-V motors in electric boat applications aims to rely on natural air-cooling systems. Therefore, it is essential to ensure that the IPM-V motor's temperature remains within safe limits during its operation, as determined through temperature simulations. Based on the operational requirements of the design, there are two operation scenarios: fishing, which has a runtime of an hour, and searching for fish, which has a runtime of two hours. Temperature simulations were conducted at two different speeds: 5,000 rpm and 6,300 rpm. The conditions for the IPM-V motor's temperature simulations are as follows.

- Motor cooling : natural air
- Ambient temperature : 33 °C
- Initial temperature : 33 °C

The simulation results presented in this paper focus on critical points such as windings, stator core, rotor core, and magnets, as these factors affect winding resistance, permanent magnet demagnetization, and component lifespan. Figure 10 presents the temperature simulation results at speeds of 5,000 rpm and 6,300 rpm.

Based on the temperature simulation results, at a speed of 5,000 rpm for one hour, the highest temperature was recorded in the stator core and windings, reaching 53.59° C. The highest temperature recorded in the rotor core and permanent magnets was 47.15° C. At a speed of 6,300 rpm for one hour, the highest temperature was observed in the stator core and windings, reaching 56.62 °C. The highest temperature recorded in the rotor core and permanent magnets was 49.90 °C.

For simulations at a speed of 5,000 rpm for two hours, the highest temperature was found in the stator core and windings, reaching 59.73 °C. In the rotor core and permanent magnets, the highest temperature recorded was 54.21 °C. Finally, at a speed of 6,300 rpm for two hours, the highest temperature was

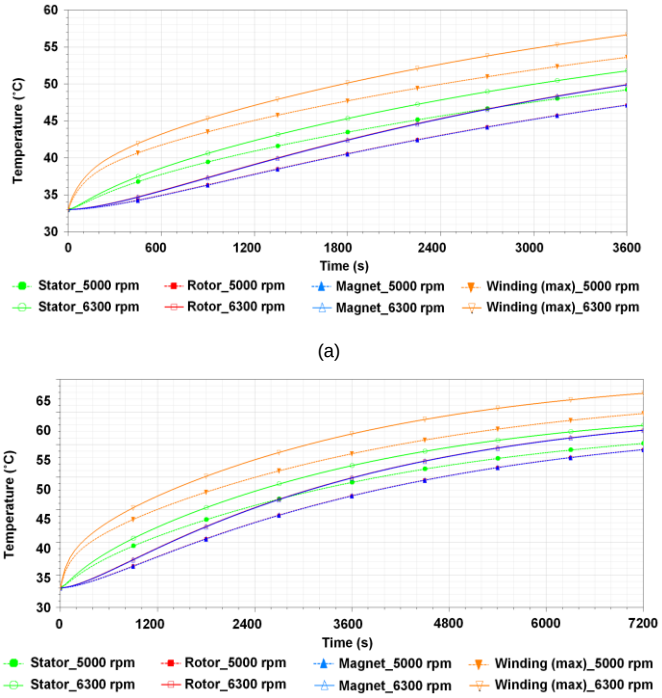

Figure 10. Temperature curve, (a) 5,000 rpm, (b) 6,300 rpm.

TABLE IV
SIMULATION RESULT SUMMARY

No	Parameter	Speed (rpm)	
		5,000	6,300
1.	Torque (Nm)	15.15	12.19
2.	Cogging torque (Nm)	1.386	
3.	Stator current (average) (A)	102.48	114.16
4.	Input power (kW)	8.82	8.95
5.	Output power (kW)	7.93	8.04
6.	Efficiency (average) (%)	89.34	88.90
7.	Stator flux density (T)	2.09	2.11
8.	Highest temperature (˚C)		
	a. One hour operation		
	- Stator and winding	53.59	56.62
	- Rotor and permanent magnet	47.15	49.90
	b. Two hours operation		
	- Stator and winding	59.73	62.83
	- Rotor and permanent magnet	54.21	57.18

observed in the stator core and windings, reaching 62.83 °C. In the rotor core and permanent magnets, the highest temperature recorded was 57.18 °C.

Based on the FEA simulation results, the condition of the IPM-V motor when operated for an hour during fishing and two hours during fish searching operations showed that the motor temperature remained below the allowed limit, in accordance with the use of class H insulation and a permanent magnet grade up to 120 °C. Table IV displays the summary of the IPM-V motor simulation results at speeds of 5,000 rpm and 6,300 rpm.

V. CONCLUSION

Ansys Maxwell FEA simulations on the electric boat IPM-V BLDC motor model examined torque, cogging torque, stator current, output power, input power, efficiency, magnetic field

distribution, and temperature. Based on these simulation results, the IPM-V BLDC motor, with an input power of 8.82 kW and an output power of 7.93 kW, could operate at 5,000 rpm, providing a torque of 15.62 Nm, and matching the set design parameters for electric boat applications. The simulations reveal an average motor power efficiency of 89% and a well-balanced stator current for smooth motor rotation.

The calculations also showed that the IPM-V BLDC motor could reach 6,300 rpm, generating 12.19 Nm of torque, 8.95 kW of input power, 8.04 kW of output power, and 88.90% of power efficiency. At 8.49% of the nominal torque, the cogging torque value obtained from the simulation was within the 10% threshold. Magnetic field distribution simulations showed safe operational limitations. According to material restrictions, the motor operates safely. The simulation results for each parameter suggest good motor quality. Nevertheless, it is crucial to verify these modelling findings through the execution of real experiments on the motor.

CONFLICTS OF INTEREST

The authors declare no conflict of interest relevant to this paper.

AUTHORS' CONTRIBUTIONS

Conceptualization, Dewi Rianti Mandasari and Cuk Supriyadi Ali Nandar; methodology, Dewi Rianti Mandasari and Budi Sudiarto; software, Dewi Rianti Mandasari; validation, Dewi Rianti Mandasari and Cuk Supriyadi Ali Nandar; investigation, Cuk Supriyadi Ali Nandar; resources, Cuk Supriyadi Ali Nandar; data curation, Dewi Rianti Mandasari and Lia Amelia; writing—original draft preparation, Dewi Rianti Mandasari and Lia Amelia; writing—review and editing, Budi Sudiarto; visualization, Dewi Rianti Mandasari; supervision, Budi Sudiarto; project administration, Lia Amelia; funding acquisition, Cuk Supriyadi Ali Nandar

ACKNOWLEDGMENT

The authors thank the National Research and Innovation Agency, Indonesia (BRIN) for supporting this research.

REFERENCES

[1] (2021) WHO global air quality guidelines: particulate matter (PM2.5 and PM10), ozone, nitrogen dioxide, sulfur dioxide and carbon monoxide, [Online], https://iris.who.int/handle/10665/345329, access date: 20-Sep-2023.

[2] (2020) State of Global Air website, [Online], https://www.stateofglobalair.org/data/#/air/plot, access date: 20-Sep-2023.

[3] N.A. Istiqomah and N.N.N. Marleni, "Particulate air pollution in Indonesia: Quality index, characteristic, and source identification," *IOP Conf. Ser., Earth Environ. Sci.*, 2020, pp. 1–8, doi: 10.1088/1755-1315/599/1/012084.

[4] (2023) Solusi untuk Polusi Udara di Jakarta, [Online], www.vitalstrategies.org/source-apportionment-report, access date: 20-Sep-2023.

[5] (2023) World Energy Balances: Overview, [Online], https://www.iea.org/reports/world-energy-balances-overview, access date: 20-Sep-2023.

[6] D. Vinezzia, "Identifikasi bahaya keselamatan dan kesehatan kerja pada aktivitas nelayan," *J. Penelit. Perawat Profesional*, vol. 3, no. 1, pp. 117–126, Feb. 2021, doi: 10.37287/jppp.v3i1.345.

[7] S.A.K.M. Niapour *et al.*, "Review of permanent-magnet brushless dc motor basic drives based on analysis and simulation study," *Int. Rev. Elect. Eng. (I.R.E.E.)*, vol. 9, no. 5, pp. 930–957, Sep./Oct 2014.

[8] A.Y. Hassan, A.G. Rohieem, and S.M.S. Salem, "Direct torque control of non-salient pole AFPMSMs with SVPWM inverter," *Int. J. Power Electron. Drive Syst. (IJPEDS)*, vol. 13, no. 4, pp. 2014–2023, Dec. 2022, doi: 10.11591/ijpeds.v13.i4.pp2014-2023.

[9] B.V.R. Kumar and K.S. Kumar, "Design of a new dual rotor radial flux BLDC motor with Halbach array magnets for an electric vehicle," *2016 IEEE Int. Conf. Power Electron. Drives Energy Syst. (PEDES)*, 2016, pp. 1–5, doi: 10.1109/PEDES.2016.7914552.

[10] M.A. Khalid *et al.*, "Performance analysis of brushless dc motor with optimum magnetic energy for bicycle application," *Int. J. Power Electron. Drive Syst. (IJPEDS)*, vol. 12, no. 4, pp. 2113–2122, Dec. 2021, doi: 10.11591/ijpeds.v12.i4.pp2113-2122.

[11] E. Elakkia, S.J. Anita, R.G. Ganesan, and S. Saikiran, "Design and modelling of BLDC motor for automotive applications," *Int. J. Elect. Electron. Eng. Telecommun.*, vol. 1, no. 1, pp. 42–48, Mar. 2015.

[12] J.M. Patel, H.V. Hirvaniya, and M. Rathod, "Simulation and analysis of brushless dc motor based on sinusoidal PWM control," *Int. J. Innov. Res. Elect. Electron. Instrum. Control Eng.*, vol. 2, no. 3, pp. 1236–1238, Mar. 2014.

[13] A. Tashakori, M. Ektesabi, and N. Hosseinzadeh, "Characteristics of suitable drive train for electric vehicle," *Int. Conf. Instrum. Meas. Circuits Syst. (ICIMCS 2011)*, 2011, pp. 535–541, doi: 10.1115/1.859902.paper119.

[14] H. Kim and B. Kwon, "Optimal design of motor shape and magnetisation direction to obtain vibration reduction and average torque improvement in IPM BLDC motor," *IET Elect. Power Appl.*, vol. 11, no. 3, pp. 378–385, Mar. 2017, doi: 10.1049/iet-epa.2016.0618.

[15] J. Hur and B.-W. Kim, "Rotor shape design of an interior PM type BLDC motor for improving mechanical vibration and EMI characteristics," *J. Elect. Eng. Technol.*, vol. 5, no. 3, pp. 462–467, Sep. 2010, doi: 10.5370/JEET.2010.5.3.462.

[16] C. He and T. Wu, "Permanent magnet brushless dc motor and mechanical structure design for the electric impact wrench system," *Energies*, vol. 11, no. 6, pp. 1–24, Jun. 2018, doi: 10.3390/en11061360.

[17] K.F. Rahmantya *et al.*, "Kelautan dan perikanan dalam angka tahun 2022," The Center for Data, Statistics and Information, The Ministry of Marine Affairs and Fisheries, Jakarta, Indonesia, 2022, vol. 1.

[18] *Yamaha 9.9c 15c Service Manual*, Yamaha Motor Corporation, Cypress, CA, USA, 2003.

[19] X. Liu, H. Chen, J. Zhao, and A. Belahcen, "Research on the performances and parameters of interior PMSM used for electric vehicles," *IEEE Trans. Ind. Electron.*, vol. 63, no. 6, pp. 3533–3545, Jun. 2016, doi: 10.1109/TIE.2016.2524415.

[20] Safril *et al.*, "Design of cooling system on brushless dc motor to improve heat transfers efficiency," *Evergreen*, vol. 9, no. 2, pp. 584–593, Jun. 2022, doi: 10.5109/4794206.

[21] J. Kuria and P. Hwang, "Investigation of thermal performance of electric vehicle BLDC motor," *Int. J. Mech. Eng.*, vol. 1, no. 1, pp. 1–17, 2012.

[22] J. Dong, Y. Huang, L. Jin, and H. Lin, "Comparative study of surface-mounted and interior permanent-magnet motors for high-speed applications," *IEEE Trans. Appl. Supercond.*, vol. 26, no. 4, pp. 1–4, Jun. 2016, doi: 10.1109/TASC.2016.2514342.

[23] H.-I. Park, J.-Y. Choi, K.-H. Jeong, and S.-K. Cho, "Comparative analysis of surface-mounted and interior permanent magnet synchronous motor for compressor of air-conditioning system in electric vehicles," *2015 9th Int. Conf. Power Electron. ECCE Asia (ICPE-ECCE Asia)*, 2015, pp. 1700–1705, doi: 10.1109/ICPE.2015.7168006.

[24] Z.Q. Zhu and Y.X. Li, "Modularity techniques in high performance permanent magnet machines and applications," *CES Trans. Elect. Mach. Syst.*, vol. 2, no. 1, pp. 93–103, Mar. 2018, doi: 10.23919/TEMS.2018.8326455.

[25] Y. Yang *et al.*, "Design and comparison of interior permanent magnet motor topologies for traction applications," *IEEE Trans. Transp. Electrific.*, vol. 3, no. 1, pp. 86–97, Mar. 2017, doi: 10.1109/TTE.2016.2614972.

[26] S. Li, W. Tong, S. Wu, and R. Tang, "Analytical model for electromagnetic performance prediction of IPM motors considering different rotor topologies," *IEEE Trans. Ind. Appl.*, vol. 59, no. 4, pp. 4045–4055, Jul./Aug. 2023, doi: 10.1109/TIA.2023.3268639.

[27] D.C. Hanselman, *Brushless Permanent Magnet Motor Design*, Cranston, RI, USA: The Writers' Collective, 2003.

[28] Y. Guo *et al.*, "Parameter determination and performance analysis of a PM synchronous generator by magnetic field finite element analysis," *2007 Australas. Univ. Power Eng. Conf.*, 2007, pp. 1–4, doi: 10.1109/AUPEC.2007.4548111.

[29] W. Purwanto *et al.*, "Optimal design of stator slot geometry for high-speed spindle induction motor applications," *2019 Int. Conf. Inf. Commun.*

Technol. (ICOIACT), 2019, pp. 811–816, doi: 10.1109/ICOIACT46704.2019.8938493.

[30] J.R. Hendershot and T.J.E. Miller, *Design of Brushless Permanent-Magnet Machines*, 2nd ed. Venice, FL, USA: Motor Design Books LLC, 2010.

[31] S. Leitner, H. Gruebler, and A. Muetze, "Cogging torque minimization and performance of the sub-fractional HP BLDC claw-pole motor," *IEEE Trans. Ind. Appl.*, vol. 55, no. 5, pp. 4653–4664, Sep./Oct. 2019, doi: 10.1109/TIA.2019.2923569.

[32] M. Zhou *et al.*, "Influence of magnet shape on the cogging torque of a surface-mounted permanent magnet motor," *Chin. J. Elect. Eng.*, vol. 5, no. 4, pp. 40–50, Dec. 2019, doi: 10.23919/CJEE.2019.000026.

[33] Y. Dönmezer and L.T. Ergene, "Skewing effect on interior type BLDC motors," *The XIX Int. Conf. Elect. Mach. - ICEM 2010*, 2010, pp. 1–5, doi: 10.1109/ICELMACH.2010.5607848.

[34] D.R. Mandasari *et al.*, "Design and optimization of brushless dc motor for electric boat thruster," *Evergreen*, vol. 10, no. 3, pp. 1928–1937, Sep. 2023, doi: 10.5109/7151773.

[35] J.K. Tangudu and T.M. Jahns, "Comparison of interior PM machines with concentrated and distributed stator windings for traction applications," *2011 IEEE Vehicle Power Propuls. Conf.*, 2011, pp. 1–8, doi: 10.1109/VPPC.2011.6043171.

[36] M. Toren, "Comparatıve analysis of the magnet effects on the permanent magnet BLDC motor performance used in electric vehicles," *Elect. Eng.*, vol. 104, no. 5, pp. 3411–3423, Oct. 2022, doi: 10.1007/s00202-022-01536-1.

[37] S. Madhavan, R. Devdatta P.B, E. Gundabattini, and A. Mystkowski, "Thermal analysis and heat management strategies for an induction motor, a review," *Energies*, vol. 15, no. 21, pp. 1–20, Nov. 2022, doi: 10.3390/en15218127.

[38] F. Zhou *et al.*, "Study on steady-state temperature rise characteristics of motor heat balance under load rate," *Int. Trans. Elect. Energy Syst.*, vol. 2022, pp. 1–11, Jun. 2022, doi: 10.1155/2022/1147096.